

# Cell-Free Multi-Enzyme Synthesis and Purification of Uridine Diphosphate Galactose

Reza Mahour,<sup>[a, f]</sup> Ju Weon Lee,<sup>[b]</sup> Pia Grimpe,<sup>[a]</sup> Simon Boecker,<sup>[c]</sup> Valerian Grote,<sup>[a]</sup> Steffen Klamt,<sup>[c]</sup> Andreas Seidel-Morgenstern,<sup>[b, d]</sup> Thomas F. T. Rexer,<sup>\*, [a]</sup> and Udo Reichl<sup>[a, e]</sup>

High costs and low availability of UDP-galactose hampers the enzymatic synthesis of valuable oligosaccharides such as human milk oligosaccharides. Here, we report the development of a platform for the scalable, biocatalytic synthesis and purification of UDP-galactose. UDP-galactose was produced with a titer of 48 mM (27.2 g/L) in a small-scale batch process (200  $\mu$ L) within 24 h using 0.02  $\text{g}_{\text{enzyme}}/\text{g}_{\text{product}}$ . Through *in-situ* ATP regeneration, the amount of ATP (0.6 mM) supplemented was around 240-fold lower than the stoichiometric equivalent required to achieve the final product yield. Chromatographic purification

using porous graphic carbon adsorbent yielded UDP-galactose with a purity of 92%. The synthesis was transferred to 1 L preparative scale production in a stirred tank bioreactor. To further reduce the synthesis costs here, the supernatant of cell lysates was used bypassing expensive purification of enzymes. Here, 23.4 g/L UDP-galactose were produced within 23 h with a synthesis yield of 71% and a biocatalyst load of 0.05  $\text{g}_{\text{total\_protein}}/\text{g}_{\text{product}}$ . The costs for substrates per gram of UDP-galactose synthesized were around 0.26 €/g.

## Introduction

There is an accumulating body of knowledge documenting the positive impact of human milk oligosaccharides (HMOs) on the cognitive and physical development of infants.<sup>[1]</sup> So far, around 200 different HMO structures have been identified in human milk.<sup>[2]</sup> As these oligosaccharides are in nature exclusively synthesized in the human mammary gland, there is expanding interest in academia to synthesize well-defined structures to elucidate their specific functions.<sup>[3]</sup> Since 2016, the first synthe-

tically produced HMOs have been added to premium infant formula and there are intensive endeavors to efficiently produce the most abundant HMOs for inclusion in infant formula.<sup>[4]</sup> So far, the large scale production of HMOs relies on the fermentation of genetically engineered *Escherichia coli* strains.<sup>[3,5]</sup> However, by the consequent use of enzymatic syntheses, the scope of HMOs available in gram amounts could be much greater, especially for complex oligosaccharides.<sup>[2,6]</sup> This concerns, in particular, syntheses using microbial Leloir glycosyltransferases (GT) due the excellent stereochemistry of reactions and the availability of enzymes.<sup>[7]</sup> However, robust and scalable biocatalytic processes for the synthesis of oligosaccharides are lacking. And, in addition, high costs of nucleotide sugars as substrates for Leloir GT-catalyzed reactions have also averted the implementation of large-scale enzymatic production processes.<sup>[8]</sup>

Along fucose, sialic acid and *N*-actelyglucosamine, the carbohydrate galactose (Gal) is one of the major monosaccharide building blocks of HMOs and many other functional oligosaccharides.<sup>[1a]</sup> Uridine diphosphate galactose (UDP-Gal) is the activated form of Gal, which serves as the Gal donor in Leloir GT-catalyzed galactosylation reactions. UDP-Gal is currently only available at costs of around 170 € per 100 mg in amounts typically not exceeding 250 mg. Until recently, enzymatic synthesis of UDP-Gal relied mainly on epimerase using UDP-glucose (UDP-Glc) as substrate.<sup>[9]</sup> Zou *et al.* synthesized UDP-Gal by exploiting the promiscuity of the uridine diphosphate sugar pyrophosphorylase from Gal, adenosine triphosphate (ATP) and uridine triphosphate (UTP) bypassing the need for high-cost UDP-Glc supplementation or *in-situ* UDP-Glc synthesis and, thus, significantly simplifying the enzymatic synthesis.<sup>[10]</sup>

However, these multi-enzyme systems rely on the supplementation of catalytic amounts of expensive glucose 1-phosphate (Glc-1P). Moreover, only titers below 6 g/L UDP-Gal

[a] R. Mahour, P. Grimpe, V. Grote, T. F. T. Rexer, U. Reichl  
Max Planck Institute for Dynamics of Complex Technical Systems,  
Department of Bioprocess Engineering  
Sandtorstrasse 1, 39106 Magdeburg (Germany)  
E-mail: rexer@mpi-magdeburg.mpg.de


[b] J. W. Lee, A. Seidel-Morgenstern  
Max Planck Institute for Dynamics of Complex Technical Systems,  
Department of Physical and Chemical Foundations of Process Engineering  
Sandtorstrasse 1, 39106 Magdeburg (Germany)


[c] S. Boecker, S. Klamt  
Max Planck Institute for Dynamics of Complex Technical Systems,  
Research group Analysis and Redesign of Biological Networks  
Sandtorstrasse 1, 39106 Magdeburg (Germany)

[d] A. Seidel-Morgenstern  
Otto-von-Guericke University Magdeburg,  
Chair of Chemical Process Engineering  
Universitätsplatz 2, 39106 Magdeburg (Germany)

[e] U. Reichl  
Otto-von-Guericke University Magdeburg,  
Chair of Bioprocess Engineering  
Universitätsplatz 2, 39106 Magdeburg (Germany)

[f] R. Mahour  
Present Address: c-Lecta GmbH, Leipzig (Germany)

 Supporting information for this article is available on the WWW under <https://doi.org/10.1002/cbic.202100361>

 © 2021 The Authors. ChemBioChem published by Wiley-VCH GmbH. This is an open access article under the terms of the Creative Commons Attribution Non-Commercial License, which permits use, distribution and reproduction in any medium, provided the original work is properly cited and is not used for commercial purposes.

have been achieved and the scalability to larger batch volumes has not been demonstrated.<sup>[9b,11]</sup>

Along the rational design of pathways, for which new computer-aided tools have recently become available, high yields of active, recombinant enzymes in low-cost microbial production systems with low enzyme loads – mass of protein per mass of target product – are of paramount importance for efficient synthesis.<sup>[7b,12]</sup> Moreover, bottlenecks in multi-enzyme pathways can be remodeled by protein engineering.<sup>[13]</sup> In addition to studies demonstrating the advantages of the establishment of cell-free cascades, many reviews on the development and applications of multi-enzyme systems for the synthesis of valuable compounds have been published recently.<sup>[14]</sup>

Here, we constructed a cell-free cascade of six recombinant enzymes comprising seven reactions for synthesis of UDP-Gal, from the low-cost substrates uridine (Uri), Gal, polyphosphate (PolyP<sub>n</sub>), and catalytic amounts of ATP (Figure 1). ATP is *in-situ* regenerated from PolyP<sub>n</sub>. Furthermore, we optimized this system to achieve high product yields and lowered synthesis costs. Eventually, the optimized process was transferred from 200 μL scale to 1 L scale. For the purification of UDP-Gal, a chromatographic protocol using porous graphitic carbon (PGC) was established.

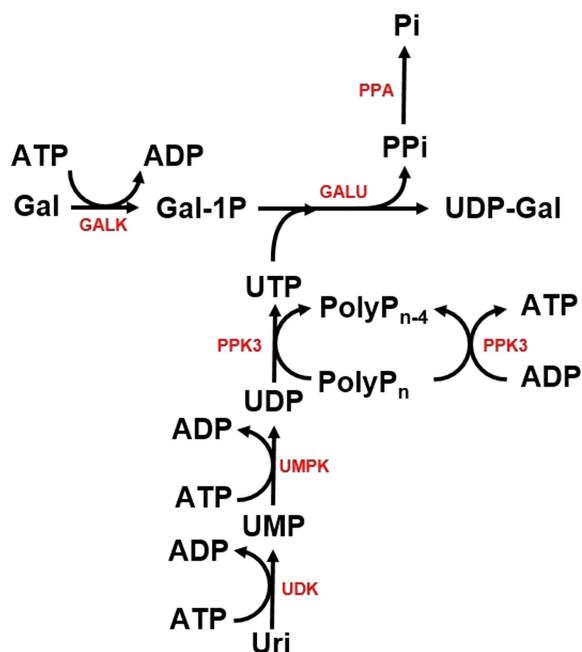


**Figure 1.** Schematic representation of UDP-Gal synthesis from Uri, Gal, PolyP<sub>n</sub> and a catalytic amount of ATP. Regeneration of ATP from ADP is achieved by exploiting the promiscuity of PPK3 toward diphosphate nucleotides. The enzyme names are as follows: UDK, Uridine-cytidine kinase; UMPK, UMP kinase; PPK3, Polyphosphate kinase; GALK, Galactokinase; GALU, UTP-glucose-1-phosphate uridylyltransferase; PPA, Inorganic diphosphatase.

## Results and Discussion

### Development of the cell-free cascade

An extensive literature research was conducted to select suitable enzymes for the production of UDP-Gal from Gal, Uri, PolyP<sub>n</sub>, and (small amounts) of ATP. Criteria employed were activity and overlapping pH and temperature ranges.<sup>[15]</sup> The selected enzymes and their activity ranges are detailed in the experimental section. A scheme of the established cascade is depicted in Figure 1. To facilitate the *in-situ* regeneration of ATP from ADP and PolyP<sub>n</sub>, a regeneration cycle was implemented by exploiting the promiscuity of PPK3 toward diphosphate nucleotides. Hence, in our system, the PPK3 phosphorylates UDP and ADP consuming PolyP<sub>n</sub>. It was reported that the recombinant protein GALU (from *E. coli*) has a broad substrate promiscuity towards phosphorylated hexoses, such as Glc, mannose, Gal and *N*-acetylglucosamine.<sup>[16]</sup> In our work, reaction assays of GALU verified its activity towards the conversion of Gal-1P and UTP to UDP-Gal and diphosphate (Ppi) (data not shown).

### Proof-of-concept

All selected enzymes were reported to be active at pH 7.5 and, thus, this value was chosen as the initial pH for the proof-of-concept run. Concentration time course of the reactants of the one-pot multi-enzyme run are shown in Figure 2. Uri is consumed within the first hour resulting in the production of UMP, UDP, UTP, and UDP-Gal. The steady-state of the ATP and ADP concentrations after one hour, as well the production of UDP-Gal concentrations beyond the amount that initial ATP concentrations allowed, verified the functionality of the *in-situ* regeneration cycle. Overall, UDP-Gal was produced with a titer of 5.3 mM (3 g/L) and a yield of 91% from Uri and Gal within 5 h with an enzyme load of 0.09 g<sub>enzyme</sub>/g<sub>product</sub>.

### Optimization

To increase final product yields through systematic optimization of the cascade, the impact of substrate loads and co-factor concentrations as well as pH values were examined.

**Substrate load and co-factor:** To optimize the cascade with respect to yield and productivity, the impact of the co-factor concentration was examined for different initial concentrations of Uri and Gal. It comprised two sets of three independent runs with initial Uri and Gal concentrations of 20, 35 and 50 mM, respectively. The first set was supplemented with 50 mM and the second set with 75 mM MgCl<sub>2</sub>. All runs were initiated at pH 7.5 and 37 °C. The concentration time courses of all runs are shown in Figure 3.

In the first set with 50 mM MgCl<sub>2</sub> supplementation, the conversion of 20 mM Uri and Gal was completed within around 8 h with a yield approaching 100% (see Figure 3, top). Both runs with higher substrate concentrations did not result in high synthesis yields.

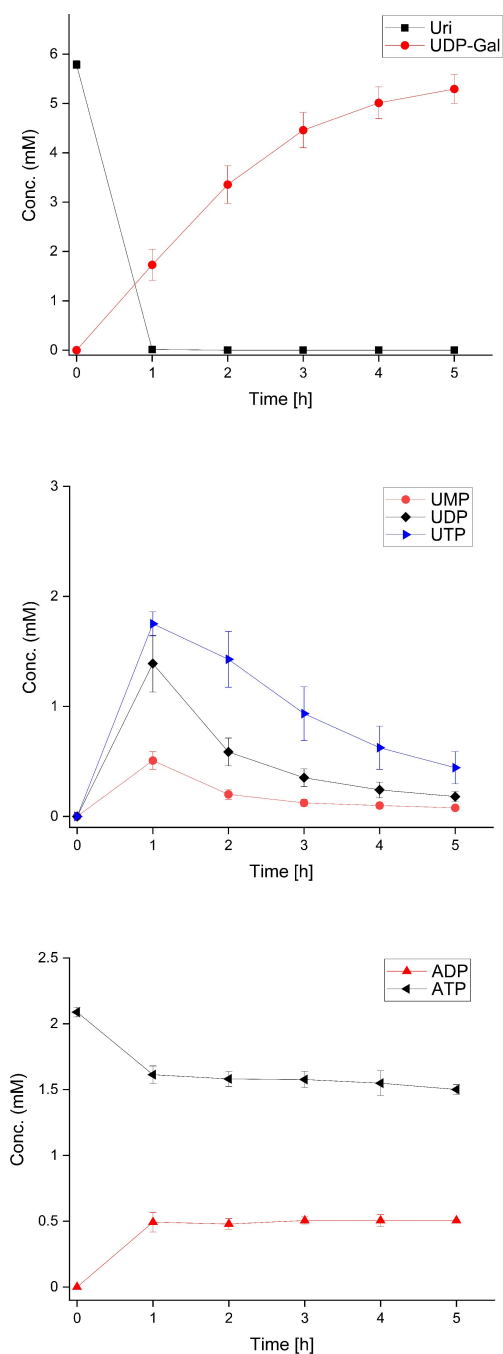


**Figure 2.** One-pot multi-enzyme synthesis of UDP-Gal. Concentration time courses for (top) Uri and UDP-Gal, (middle) UMP, UDP and UTP and (bottom) ADP and ATP. The experimental conditions: 150 mM Tris-HCl (pH 7.5), 50 mM  $MgCl_2$ , 5.8 mM Uri, 6 mM Gal, 2 mM ATP, 5 mM PolyP<sub>n</sub>, 0.04  $\mu\text{g}/\mu\text{L}$  UDK, 0.06  $\mu\text{g}/\mu\text{L}$  UMPK/PPK3, 0.05  $\mu\text{g}/\mu\text{L}$  GALK, 0.08  $\mu\text{g}/\mu\text{L}$  GALU, 0.06  $\mu\text{g}/\mu\text{L}$  PPA in a total volume of 100  $\mu\text{L}$ . The runs were carried out in triplicates; error bars represent standard deviation.

In the second set with 75 mM  $MgCl_2$  supplementation, similar results for the run starting from 20 mM Uri were obtained (see Figure 3, bottom). However, a final UDP-Gal concentration of around 30 mM (up from 15 mM for 50 mM  $MgCl_2$ ) was achieved starting from 35 mM Uri and Gal while the

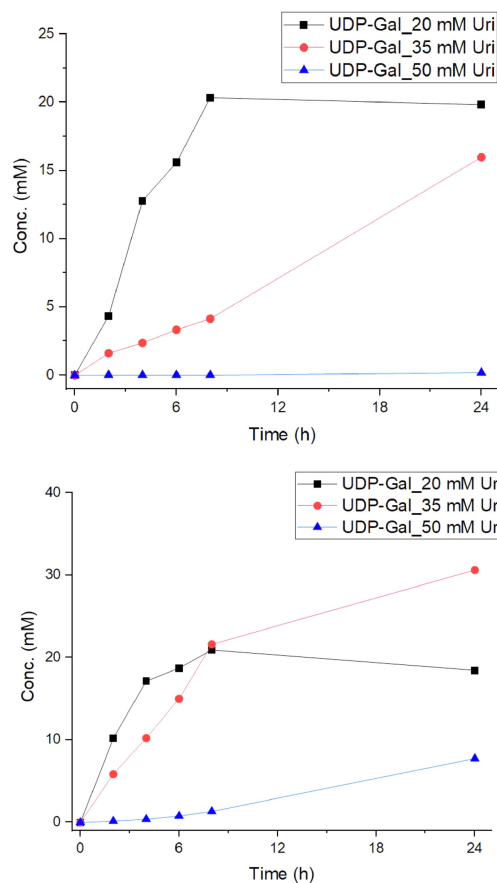


**Figure 3.** Concentration time courses for UDP-Gal synthesis with  $MgCl_2$  co-factor concentrations of (top) 50 mM and (bottom) 75 mM for initial Uri and Gal concentrations of 20, 35 and 50 mM. Enzyme concentrations for both reactions were as follows: 0.07  $\mu\text{g}/\mu\text{L}$  UDK, 0.12  $\mu\text{g}/\mu\text{L}$  UMPK/PPK3, 0.17  $\mu\text{g}/\mu\text{L}$  GAL, 0.12  $\mu\text{g}/\mu\text{L}$  GALU, 0.06  $\mu\text{g}/\mu\text{L}$  PPA in a total volume of 200  $\mu\text{L}$ .

yield of the cascade for starting concentration of 50 mM Uri (and Gal) remained low.

In a mechanistic study of polyphosphate kinase 2 by Parnell *et al.*, it was reported that binding of  $Mg^{2+}$  and PolyP<sub>n</sub> is essential for the activity of polyphosphate kinase 2. While the study was performed on a different family of polyphosphate kinase, we hypothesize that higher concentrations of  $Mg^{2+}$  can recover some of the potentially lost activity of PPK3 – and, thus, elevate the UTP concentration – by increasing  $Mg^{2+}$ -PolyP<sub>n</sub> complex formation. Another need for elevated  $Mg^{2+}$  supplementation could arise from the precipitation of  $Mg_2(PO_4)_3$  from the reaction solution.<sup>[17]</sup>

**pH value:** To optimize the pH value, five independent runs with pH values ranging from 7–9 were carried out. Initial substrate concentrations were 55 mM Gal and 53 mM Uri, and a co-factor concentration of 75 mM  $MgCl_2$  was employed. The percentage conversion after a run time of 24 h is shown in Figure 4. At pH 8.5, 44.6 mM (25.2 g/L) UDP-Gal was obtained, and this pH was selected for follow-up runs.

**Minimizing the amount of required ATP:** In comparison to Gal, Uri, and PolyP<sub>n</sub>, ATP is a comparatively expensive substrate. Thus, the minimal initial catalytic amount of ATP that can be

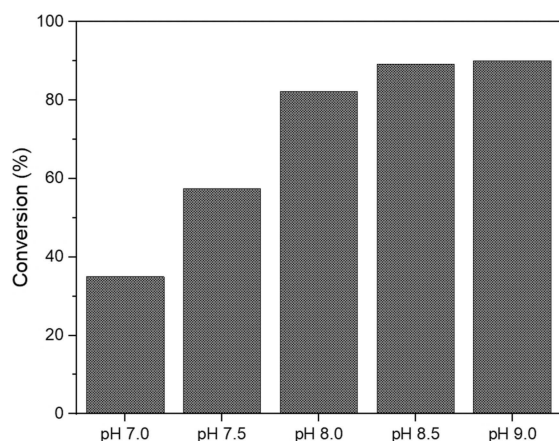


**Figure 4.** Conversion of Uri to UDP-Gal for different pH values after 24 h of incubation at 37 °C. The conversion refers to the percentage of synthesized UDP-Gal over the initial amount of Uri. The systems might not be in equilibrium after 24 h. The runs for examining different pH values were carried out in 150 mM Tris-HCl, 75 mM MgCl<sub>2</sub>, 53 mM Uri, 55 mM Gal, 2.5 mM ATP and 20 mM PolyP<sub>n</sub>. Enzyme concentrations were as follows: 0.08 µg/µL UDK, 0.14 µg/µL UMPK/PPK3, 0.21 µg/µL GALK, 0.14 µg/µL GALU, 0.08 µg/µL PPA in a total volume of 200 µL.

used without sacrificing the yield after 24 h was determined through five independent runs. The initial ATP concentrations were 0.1, 0.2, 0.6, 1.0, and 2.5 mM, respectively. The concentrations of UDP-Gal after 24 h are shown in Figure 5. Percentage conversion rates of UDP-Gal using 0.1 mM and 0.2 mM ATP with respect to the substrates were around 15% and 25%, respectively. In contrast, the runs with initial ATP concentrations of 0.6 mM, 1 mM and 2.5 mM showed almost quantitative yields. The concentration time courses of reactants for the runs using 0.6 mM ATP are shown in Figure 6. Under these conditions, UDP-Gal was produced with a final concentration of 48 mM (27.2 g/L) and a synthesis yield of 96% and 92%

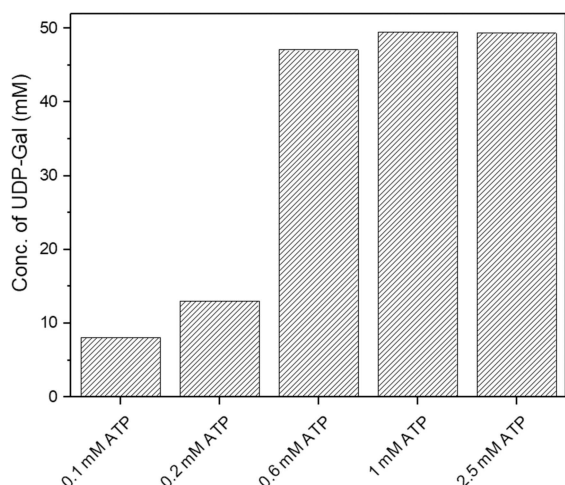


**Figure 5.** Final concentration of UDP-Gal for different initial concentrations of ATP. The runs contained 150 mM Tris-HCl (pH 8.5), 75 mM MgCl<sub>2</sub>, 50 mM Uri, 52 mM Gal, 20 mM PolyP<sub>n</sub>, 0.07 µg/µL UDK, 0.12 µg/µL UMPK/PPK3, 0.17 µg/µL GALK, 0.12 µg/µL GALU, and 0.06 µg/µL PPA in a total volume of 250 µL.

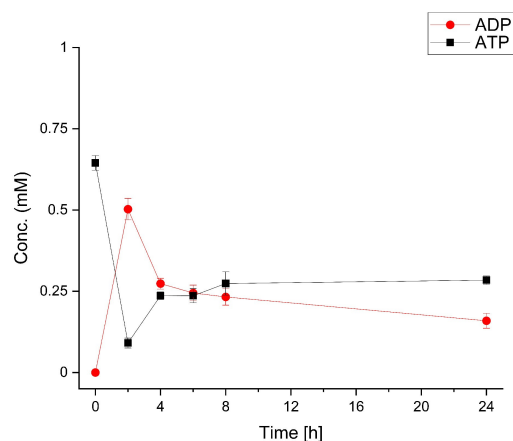
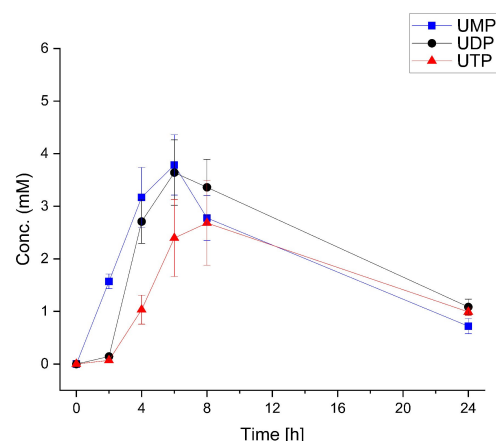
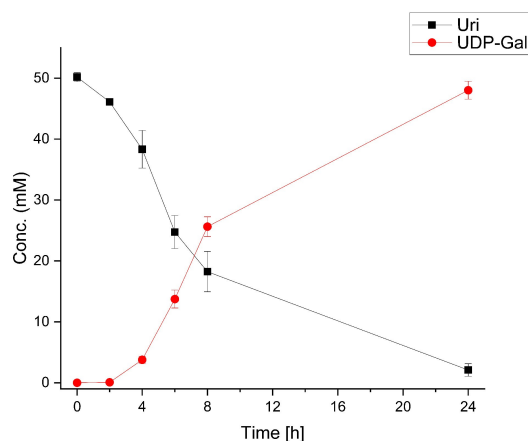


**Figure 6.** Concentration time course for synthesis of UDP-Gal under optimized conditions. (Top) concentration of Uri and UDP-Gal; (middle) concentration of UMP, UDP and UTP; (bottom) concentration of ADP and ATP. The runs contained 150 mM Tris-HCl (pH 8.5), 75 mM MgCl<sub>2</sub>, 50 mM Uri, 52 mM Gal, 20 mM PolyP<sub>n</sub>, 0.07 µg/µL UDK, 0.12 µg/µL UMPK/PPK3, 0.17 µg/µL GALK, 0.12 µg/µL GALU and 0.06 µg/µL PPA in a total volume of 250 µL. The runs were carried out in triplicate; error bars represent the standard error of the measurements.

regarding Uri and Gal, respectively. The enzyme load was 0.02 g<sub>enzyme</sub>/g<sub>product</sub> and ATP was used around 240 times less than the stoichiometric amount, i.e. the ATP pool was replenished 240 times. The HPAEC-UV (High-Performance

Anion-Exchange Chromatography with UV Detection) chromatogram of the run after 2 h and 24 h is shown in Figure 7. After 24 h, UDP-Gal is by far the major component of the cascade.

### Scale-up using cell-lysates

To demonstrate the scalability of the established cascade, synthesis was carried out at 1 L preparative scale. In addition, to further optimize the synthesis towards economic viability, the purification of enzymes was bypassed by directly using the supernatant of cell lysates after centrifugation. At first, ten runs with various enzyme loads ranging from 7.5 to 50%  $V_{\text{lysate}}/V_{\text{reaction}}$  were carried out in volumes of 200  $\mu\text{L}$  each to identify the optimal biocatalyst load. It was found that a load of 10% of  $V_{\text{lysate}}/V_{\text{reaction}}$  suffices to perform the synthesis. The same enzyme load, reaction conditions and substrate concentrations were used to perform a 1 L scale synthesis in a bioreactor with elephant ear turbine impellers (see SI). Concentration time courses of the 200  $\mu\text{L}$  and 1 L scale runs are shown in Figure 8 and show excellent agreement with small scale results confirming the scalability of the cascade. Starting from 55 mM Gal and 58 mM Uri, UDP-Gal was synthesized within 23 h with a final concentration of 41.3 mM (23.4 g/L) and a synthesis yield of 71% with respect to Uri. Due to the expected degradation of ATP and ADP to AMP by residual host cell proteins, an about ten-fold higher initial ATP concentration (6.2 mM) compared to the optimal ATP concentration (0.6 mM) when using purified proteins was used. The biocatalyst load was 0.05  $\text{g}_{\text{total protein}}/\text{g}_{\text{product}}$ . The closed mass balance for both uridine- ( $102 \pm 5\%$ ), and adenine-containing ( $108 \pm 10\%$ ) compounds during the batch time, imply that there are no significant side reactions that divest reactants from the cascade reactions.

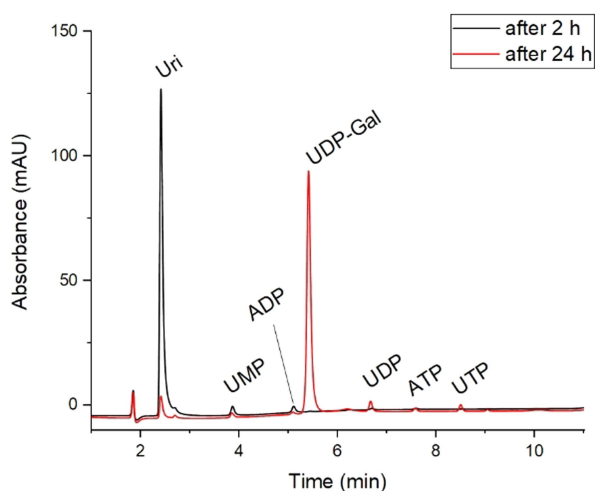


**Figure 7.** HPAEC-UV chromatogram after a reaction time of 2 h and 24 h of cascade runs using an initial ATP concentration of 0.6 mM.

### Purification

In this work, contents of acetonitrile as an organic modifier and sodium acetate (Na-Ac) as an ionic additive were adjusted in a multi-step elution mode to purify UDP-Gal after enzymatic synthesis. Analytical scale of a porous graphitic column (0.46 cm  $\times$  3.0 cm) was used for both the isolation of UDP-Gal from the reaction mixture (the 1<sup>st</sup> purification step) and capturing UDP-Gal from the 1<sup>st</sup> step fraction solution (the 2<sup>nd</sup> capture step).

Figure 9 shows the gradient chromatogram of the 1<sup>st</sup> purification step. To isolate UDP-Gal, a five-step gradient elution was applied. At the beginning, the column was equilibrated with pure water. After injecting the feed mixture (100  $\mu\text{L}$ ), the column was washed with pure water and water/acetonitrile (50/50 vol.%) to remove non-retained and non-charged impurities. To enhance the selectivity of the target component, the content of acetonitrile was reduced to 5 vol% and the concentration of sodium acetate was increased to 237.5 mM (95 vol% of 250 mM of sodium acetate). After elution of UDP-Gal, the content of acetonitrile was increased to 50 vol% to regenerate the column.

Porous graphitic carbon (PGC) adsorbents have strong interaction with  $\pi$ -bonds and ionic functional groups that can be modulated by organic solvents and ionic additives, respectively. UDP-Gal and nucleotides as unwanted impurities are not eluted with a mobile phase that contains only an organic modifier (acetonitrile) or an ionic additive (sodium acetate).<sup>[18]</sup> At the end of step 2 (6 min), the column was filled with a high content of acetonitrile (50%), so that the column had to be flushed with a low content of organic solvent (step 3) before conducting step 4 to avoid UDP-Gal losses that may be caused by radical changes of the mobile phases between the steps 2 and 4 (Figure 9).

UDP-Gal was completely recovered with a very high purity (no other components detected). However, it was diluted in the aqueous solution that contains a high concentration of sodium acetate (2.8% of the feed concentration). Under this condition, UDP-Gal rapidly degrades to UDP and galactose, cf. Table 1. To reduce the content of sodium acetate and concentrate the target compound, the same PGC column was applied to capture UDP-Gal. Figure 10 shows the 2<sup>nd</sup> capture step chromatogram of the 1<sup>st</sup> step fraction solution. The solvent composition of the 1<sup>st</sup> step fraction was too strong to capture UDP-Gal in the PGC

**Table 1.** Content of the target compound UDP-Gal and the major impurity UDP for the feed mixture and after the separation steps.

	Content		Dilution <sup>[a]</sup>	Recovery
	UDP	UDP-Gal		
Feed mixture	64%	36%	1	–
1 <sup>st</sup> step fraction (fresh) <sup>[b]</sup>	–	100%	0.028	100%
1 <sup>st</sup> step fraction (residue) <sup>[c]</sup>	26%	74%	0.025	90%
2 <sup>nd</sup> step fraction	8%	92%	0.247	87%

[a] Dilution ratio of the target compound with respect to the target concentration in the feed mixture. [b] The 1<sup>st</sup> step fraction was analyzed right after the 1<sup>st</sup> purification step. [c] The residue of the 2<sup>nd</sup> capture step feed, which is the same with the 1<sup>st</sup> step fraction was analyzed after exposing in room temperature for 2 days.

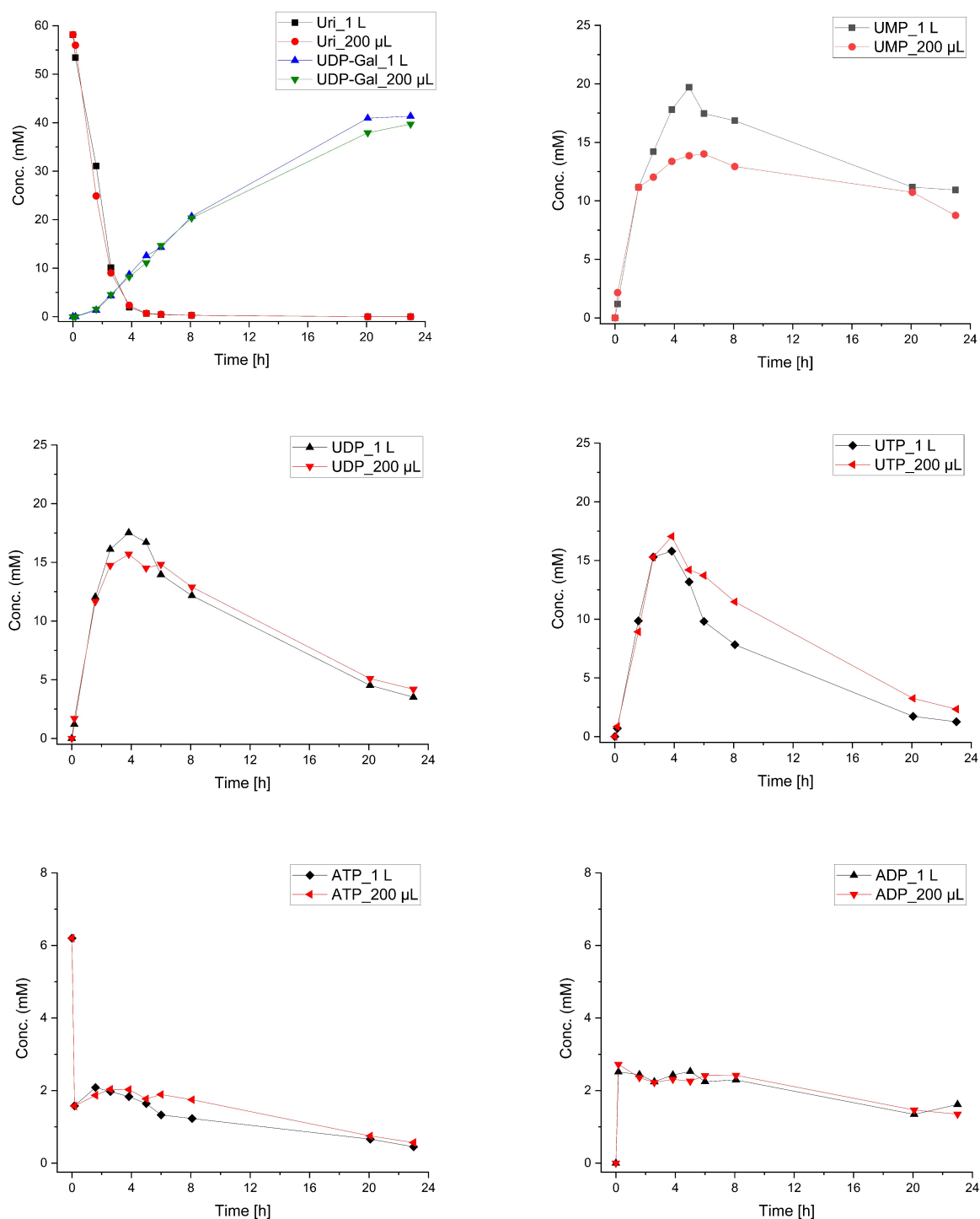


**Figure 8.** 200  $\mu\text{L}$  and 1 L scale synthesis of UDP-Gal using the supernatant from a cell lysate at 37 °C: (top) Uri and UDP-Gal; (second from top) UMP; (third from top) UDP; (third from bottom) UTP; (second from bottom) ATP; (bottom) ADP. The runs were carried out with the following conditions: 150 mM Tris-HCl (pH 8.5), 58 mM Uri, 55 mM Gal, 6.2 mM ATP, 20 mM PolyP<sub>n</sub>, and 75 mM MgCl<sub>2</sub>. The 1 L scale run was stirred with a magnetic stirrer at 60 rpm and the 200  $\mu\text{L}$  scale run was stirred at 550 rpm in a thermomixer.

column, so that it should be diluted with pure water. At the beginning, 4 mL of the 1<sup>st</sup> step fraction solution was loaded for 20 min diluting with water (10 vol% of the 1<sup>st</sup> step fraction solution and 90 vol% of water). After washing with pure water for 1 min, captured UDP-Gal eluted from the PGC column with

25 mM of sodium acetate and 50 vol% of acetonitrile (2<sup>nd</sup> step fraction). The concentration of UDP-Gal in the 2<sup>nd</sup> step fraction was 8.8 times higher than the 1<sup>st</sup> step fraction (24.7% of the feed concentration), and the concentration of sodium acetate

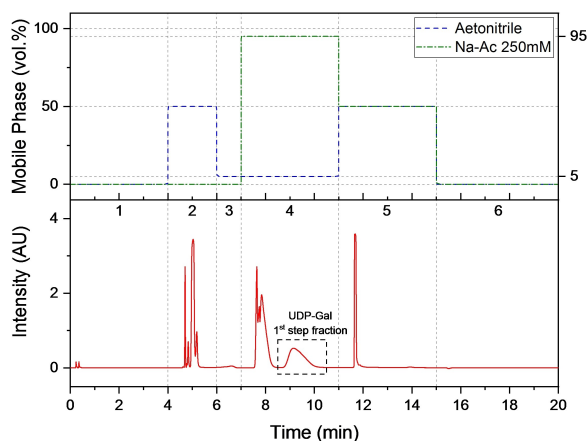


**Figure 9.** Gradient chromatogram of the 1<sup>st</sup> step purification step. UDP-Gal was fractionated from 8.8 min to 10.8 min (4 mL). Mobile phases: water (omitted)/acetonitrile/sodium acetate (Na-Ac); flow-rate: 2.0 mL/min; numbers above chromatogram indicate gradient steps.

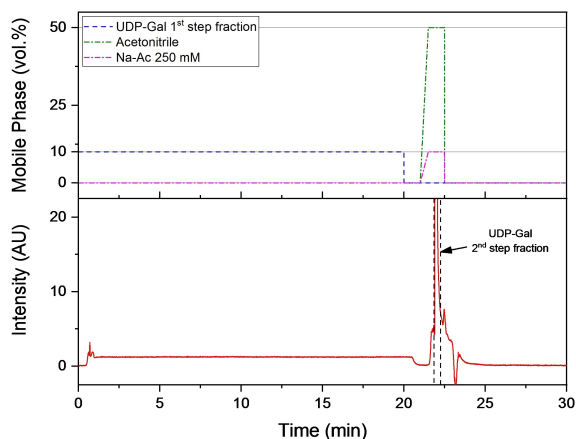


**Figure 10.** Capture chromatogram of the 1<sup>st</sup> step fraction solution. 4 mL of the 1<sup>st</sup> step fraction solution was fed, and the concentrated UDP-Gal was fractionated for 0.2 min. Mobile phases: water (omitted)/UDP-Gal 1<sup>st</sup> step fraction/acetonitrile/sodium acetate (Na-Ac); flow-rate: 2.0 mL/min.

was decreased to 25 mM. The recovery of UDP-Gal through the two-step purification was 87% with 92% of purity.

## Discussion

Several studies on the enzymatic synthesis of UDP-Gal have been previously published (see Table 2).

Koizumi *et al.* developed a process using permeabilized engineered microbial cells for large scale production of UDP-Gal.<sup>[19]</sup> A titer of 44 g/L of UDP-Gal was obtained with yields of 78% and 19% from orotic acid and Gal, respectively. While the precursors used are inexpensive, the product yield is the highest reported in literature. The high concentration of cells (200 g/L of cells, biocatalyst load 4.5 g<sub>biocatalyst</sub>/g<sub>product</sub>) used for UDP-Gal synthesis renders a large-scale implementation difficult.

In another multi-enzyme approach, UDP-Gal was synthesized in a repetitive batch mode in gram scale from UDP-Glc, Gal-1P, and nicotinamide adenine dinucleotide (NADP) with a yield of 75% with respect to UDP-Glc.<sup>[9a]</sup> However, UDP-Glc (65 €/g) and NADP (18 €/g) are high-cost substrates, which potentially prevents large-scale implementation of this process. Later, the approach was improved by Fischöder *et al.* using Gal, ATP, and UTP as substrates.<sup>[20]</sup> In a batch time of 0.5 h and a volume of 20 mL, a UDP-Gal titer of 7.1 g/L was achieved.

Moreover, Liu *et al.*, established a system of seven enzymes to produce UDP-Gal from UMP, Gal, PolyP<sub>n</sub>, and catalytic amounts of ATP, Glc-1P, and UDP-Glc.<sup>[9b]</sup> PolyP<sub>n</sub> was used as the phosphate source for the regeneration of ATP from ADP. Under optimized conditions, where enzymes were immobilized on agarose beads, a final titer of 3.9 g/L (35% with respect to UMP and Gal) were obtained. The same synthesis route, except using acetylphosphate instead of PolyP<sub>n</sub> for the regeneration of ATP, was used by Lee *et al.* in a batch process (100 μL), a final titer of 5.4 g/L (95% conversion) using crude extracts of six enzymes.<sup>[11]</sup>

The main objective of this study was to develop a scalable biocatalytic process for the synthesis of UDP-Gal in multi-gram amounts that is economically viable. This encompasses the utilization of inexpensive substrates available in bulk amounts as well as significantly enhanced titers compared to previous studies (> 20 g/L). Uri is the raw material for the production of UMP, which is extensively used in infant food formula and pharmaceutical applications, and available at costs of 270 €/kg.<sup>[21]</sup> Uri is typically produced by fermentation using a mutant of a *Bacillus subtilis* strain in 6000 L bioreactors with titers of 65 g/L.<sup>[22]</sup> Interestingly, recent advances in *E. coli*-based fermentations show similar performance (titers of 70.3 g/L).<sup>[23]</sup> Lactose, the precursor for the production of Gal, is a by-product in the dairy industry and available in multi-ton scales.<sup>[24]</sup> Gal is produced by enzymatic hydrolysis of lactose using galactosidases and available at costs of around 70 €/kg. Sodium polyphosphates are widely used in the food industry as additives and available at costs of around 50 €/kg (Merck).

Overall, there are three ATP-dependent kinase reactions in the designed pathway (Figure 1). Consequently, for equimolar concentrations of Uri and Gal, three times more ATP is required for stoichiometric turnover. Despite the broad availability of ATP, it is still comparatively expensive (370 €/kg) and its stoichiometric usage in the cascade would lead to high synthesis costs. Here, a previously described *in-situ* enzymatic ATP regeneration module utilizing *Ruegeria pomeroyi* PPK3 and inexpensive PolyP<sub>n</sub> was employed.<sup>[16a]</sup> Through optimization, the amounts of ATP supplementation could be reduced to 0.6 mM which is around 240 less than what is required for complete turnover of Uri and Gal without ATP regeneration. With respect to the substrate costs, this results in a cost reduction of about 66%.

To purify UDP-Gal from the reaction mix, a chromatographic purification protocol was established. In chromatographic separation, various types of activated carbons have been used as an adsorbent for decolorization and adsorption of unwanted aromatic compounds.<sup>[25]</sup> Recently, PGC was developed as an chromatographic adsorbent.<sup>[26]</sup> Its graphitic surface can enhance

**Table 2.** Summary of UDP-Gal synthesis described in literature based on whole cell and multi-enzyme catalysis.

Precursors Stoichiometric	Catalytic	P <sub>i</sub> source	Titer [g/L]	Reaction time [h]	Conversion [%]	Biocatalyst	Operation	Reaction conditions	Scale [mL]	Ref.
110 mM orotic acid, 250 mM Gal, 666 mM Glc			44	21	78	Combination of two engineered <i>E. coli</i> strains, 200 g/L	Batch	15 g/L KH <sub>2</sub> PO <sub>4</sub> , pH 7.2, 5 g/L MgSO <sub>4</sub> ·7H <sub>2</sub> O; 32 °C	2500	[19]
2.1 mM UDP-Glc, 2.8 mM Gal-1P, 2.5 mM NADP, 500 mM su- crose			1.2	2.3 (per batch)	75	3 purified enzymes	Repetitive batch; 16 batch cycles	50 mM Tris-acetate, pH 7.7, 2 mM MgSO <sub>4</sub> , 37 °C	100	[9a]
20 mM Gal, 20 mM UMP	2 mM ATP; 2 mM Glc-1P	2% w/v PolyP <sub>n</sub>	3.9	24	35	7 immobilized en- zymes	Circulation via packed bed column	50 mM Tris-HCl pH 7.4, 10 mM KCl, 10 mM MgCl <sub>2</sub> , 37 °C	200	[9b]
12 mM Gal, 10 mM UMP	1 mM ATP; 2 mM Glc-1P	40 mM acetyl phosphate	5.4	7	95	<i>E. coli</i> extract of 6 different enzymes	Batch	50 mM Tris-HCl, pH 7.5, 5 mM MgCl <sub>2</sub> , 37 °C	0.1	[11]
10 mM Gal, 10 mM ATP, 10 mM UTP			7.1	0.5 (per batch)	95	3 purified enzymes Overall 1.3 g/L	Repetitive batch	50 mM Tris-HCl, pH 7.5, 20 mM MgCl <sub>2</sub> , 37 °C	20	[20]
50 mM Uri, 52 mM Gal	0.6 mM ATP	20 mM PolyP <sub>n</sub>	27.2	24	96	6 purified enzymes Overall 0.5 g/L	Batch	150 mM Tris-HCl, pH 8.5, 75 mM MgCl <sub>2</sub> , 37 °C	0.25	This work
58 mM Uri, 55 mM Gal	2.5 mM ATP	20 mM PolyP <sub>n</sub>	23.4	23	71	6 unpurified en- zymes, Overall 0.5 g/L	Batch	150 mM Tris-HCl, pH 8.5, 75 mM MgCl <sub>2</sub> , 37 °C	1000	This work

The costs of the compounds are as follows: orotic acid ~1 €/g; Uri and UTP ~6 €/g.

adsorption power by van der Waals,  $\pi$ - $\pi$  interaction and charge-induced interaction, so that it can interact with various analytes, nonpolar olefins, aromatic compounds and ionic compounds.<sup>[18]</sup> Moreover, pure carbon adsorbents are known for their high thermal and chemical stability (> 100 °C, pH 1–14). Therefore, various analytical methods were developed with PGC columns.<sup>[27]</sup> Here, after filtration and centrifugation, the final reactor effluent contains several nucleotides (AMP, ADP, ATP, UMP and UDP) and UDP-Gal, the target compound. Nucleotides and its derivative, UDP-Gal contain aromatic rings (adenine and uracil) and ionizable phosphate functional groups, so that the porous graphitic carbon column could successfully be used to purify the target compound. Nevertheless, the high synthesis yield achieved in this work, could in future also be exploited to develop a chromatography-free downstream protocol to further reduce purification costs by sacrificing product purity.<sup>[28]</sup>

Moreover, the chromatographic purification of enzymes is a significant cost factor in cell-free biocatalytic synthesis. Here, we could successfully use the supernatant from cell lysates containing the overexpressed enzymes. The yield after a batch time of around 24 h decreased from > 90% to 71% when using the supernatant from cell lysates compared to using purified enzymes. However, the *in-situ* ATP regeneration was still intact and a concentration of 6.2 mM, around 26 times less than the concentration needed for full turnover of the substrates without the regeneration cycle, was employed. Moreover, this synthesis could be transferred from laboratory scale into a 1 L scale. The similar dynamics of each intermediates at 200  $\mu$ L and 1 L scales, illustrates that  $\mu$ L scale runs are useful scale-down models for establishment and development of multi-enzyme reaction systems for the efficient production of nucleotide sugars.

Beyond its application for the synthesis of HMOs and other functional oligosaccharides, UDP-Gal and other nucleotide sugars are also of special interest as substrates in the expanding field of enzymatic modification of glycoproteins.<sup>[7a,29]</sup>

## Conclusion

A platform was developed for the synthesis of UDP-Gal from low-cost and readily available precursors. It comprises a cell-free cascade of six enzymes involving seven reactions and subsequent chromatographic purification using a porous graphitic carbon adsorbent. Provision of stoichiometric amounts of expensive ATP was circumvented by implementing and improving an *in-situ* ATP regeneration module. The overall process was optimized for efficiency by bypassing time-consuming and expensive enzyme purification steps followed by a scale-up into a 1 L bioreactor. Here, within 23 h, a total of 23.4 g/L of UDP-Gal can be produced. Costs for substrates per gram of UDP-Gal synthesized were 0.26 €/g. Overall, the developed cascade facilitates large-scale and inexpensive production of UDP-Gal. In the future, the availability of low-cost UDP-Gal will eventually support the cell-free, enzymatic galactosylation of functional oligosaccharide like HMOs and *N*-glycans of therapeutic proteins.

## Experimental Section

The chemicals and protocols for strain preparation, gene expression and reaction analytics used are detailed in the supporting



information (SI). Compound prices are from the online catalogue of Carbosynth Ltd., except for PolyP<sub>n</sub> (Merck, Germany) in 2020. The PolyP<sub>n</sub> concentration refers to the concentration of polyphosphate molecules but not the phosphate units.

### Enzyme production

The *E. coli* LOBSTR strain (Kerafast, USA) was used for the production of recombinant enzymes. Strains harboring plasmids were incubated in Lysogeny broth (LB) and Terrific broth (TB), respectively. Cells were grown at 37 °C to an OD<sub>600</sub> of 0.8–1 followed by induction using 0.4 mM Isopropyl β-D-1-thiogalactopyranoside (IPTG) and gene expression for 20 h at 16 °C. The biomass was harvested by centrifugation followed by cell lysis employing high-pressure homogenization (Maximotor, Switzerland). Enzymes were purified by immobilized metal affinity chromatography (IMAC) employing an ÄKTA start instrument (GE Healthcare Life Sciences, Uppsala, Sweden) equipped with 5 mL HisTrap FF columns (GE Healthcare Life Sciences, Uppsala, Sweden). Therefore, fractions containing the protein of interest were pooled and the buffer was exchanged by using Amicon® Ultra-15 Centrifugal Filter Unit – 3 KDa MW cut-off (Merck, Germany). Concentrated enzyme stock solutions were mixed 1:1 with glycerol for storage at –20 °C. For more details on gene inserts, vectors and buffer concentrations see SI.

### Cell-free synthesis

All small-scale cascade runs were performed in 1.5 mL Eppendorf safe-lock tubes (Eppendorf, Germany) at 37 °C and 550 rpm rotational shaking in Eppendorf Thermomixer comfort (Eppendorf, Germany), unless stated otherwise. For concentration time courses, aliquots were taken and quenched into 90 °C MiliQ water for 3 minutes.

**Proof-of-concept experiment:** All runs to demonstrate the successful operation of the cascade were carried out in 150 mM Tris-HCl (pH 7.5), 50 mM MgCl<sub>2</sub>, 5.8 mM Uri, 6 mM Gal, 2 mM ATP, 5 mM PolyP<sub>nr</sub>, 0.04 μg/μL UDK, 0.06 μg/μL UMPK/PPK3, 0.05 μg/μL GALK, 0.08 μg/μL GALU, and 0.06 μg/μL PPA in a total volume of 100 μL. The runs were carried out in triplicates.

**Optimization: substrate load and co-factor:** All runs for investigating the substrate load of the cascade were carried out in 150 mM Tris-HCl (pH 7.5). Each of the runs contained 50 mM MgCl<sub>2</sub>, 0.07 μg/μL UDK, 0.12 μg/μL UMPK/PPK3, 0.17 μg/μL GALK, 0.12 μg/μL GALU and 0.06 μg/μL PPA in a total volume of 200 μL. Tested substrate concentrations were 20 mM Uri, 20 mM Gal, 3.7 mM ATP, 10 mM PolyP<sub>nr</sub>, 35 mM Uri, 35 mM Gal, 7.3 mM ATP, 17.5 mM PolyP<sub>nr</sub>, 50 mM Uri, 50 mM Gal, 11 mM ATP, and 25 mM PolyP<sub>n</sub>. To evaluate the role of co-factor concentration, the same set of runs was repeated with 75 mM MgCl<sub>2</sub>.

**Optimization: pH values:** All runs for testing different pH values were carried out in 150 mM Tris-HCl with a co-factor concentration of 75 mM MgCl<sub>2</sub>. The tested pH values were 7.0, 7.5, 8.0, 8.5, and 9.0. Each of the runs contained 53 mM Uri, 55 mM Gal, 2.5 mM ATP, 20 mM PolyP<sub>nr</sub>, 0.08 μg/μL UDK, 0.14 μg/μL UMPK/PPK3, 0.21 μg/μL GALK, 0.14 μg/μL GALU, and 0.08 μg/μL PPA in a total volume of 200 μL.

**Optimization: minimizing the amount of required ATP:** Five sets of runs with ATP concentrations of 0.1, 0.2, 0.5, 1.0, and 2.5 mM were carried out. Each run contained 150 mM Tris-HCl (pH 8.5), 75 mM MgCl<sub>2</sub>, 50 mM Uri, 52 mM Gal, 20 mM PolyP<sub>nr</sub>, 0.07 μg/μL UDK, 0.12 μg/μL UMPK/PPK3, 0.17 μg/μL GALK, 0.12 μg/μL GALU, and 0.06 μg/μL PPA in a total volume of 250 μL.

**Scale-up (1 L):** The run was carried out in a spinner flask (1.5 L) (see SI) with Elephant ear turbine impellers (DASGIP, Germany) in a volume of 1 L. The rationale for selecting the latter over standard impellers such as Rushton turbine impellers, was the lower associated shear rate.<sup>[30]</sup> The cell lysate – without any purification step – was used directly for the synthesis. For the preparation of the biocatalyst mix the following biomasses each from 200 mL cultivation, except for PPA which was 45 mL, were mixed: UDK, 3.46 g; UMPK/PPK3, 5.2 g; GALK, 5.54 g; GALU, 5.7 g; PPA, 1.7 g in 120 mL of 50 mM HEPES buffer (pH 8.1), 400 mM NaCl and 5% glycerol. The mixture was passed three times through a high-pressure homogenizer (Maximotor, Switzerland). The cell-free extract was centrifuged at 11,000 × g for 45 min. Small scale (200 μL) scouting runs were carried out to identify a suitable biocatalyst amount for the UDP-Gal synthesis. The synthesis conditions were as follows: 150 mM Tris-HCl (pH 8.5), 58 mM Uri, 55 mM Gal, 6.2 mM ATP, 20 mM PolyP<sub>nr</sub>, and 75 mM MgCl<sub>2</sub>. The run was carried out at 37 °C and 60 rpm (magnetic stirrer).

### Purification

The PGC column, Hypercarb (5 μm, 4.6 × 30 mm, Thermo Fisher, USA) was used with the Ultra 3000 High performance liquid chromatography (HPLC) system (Thermo Fisher, USA) comprising a 4-channel HPLC pump, an auto sampler, a column oven and a photo diode array detector. Deionized water, acetonitrile, and 250 mM of sodium acetate solution, in which 10 g/L of sodium hydroxide and 15 g/L of acetic acid were dissolved, were used as the mobile phase. The column temperature was set to 40 °C and the mobile phase flow-rate was fixed to 2 mL/min.

### Acknowledgements

The authors would like to thank Anja Bastian, Lisa Fichtmueller and Barbara Koehler for technical support and Felipe Tapia and Yvonne Genzel for help with the bioreactor. Open Access funding enabled and organized by Projekt DEAL.

### Conflict of Interest

R.M. and T.F.T.R. are the inventors of a pending patent on the described topic.

**Keywords:** ATP regeneration · cell-free synthesis · multi-enzymes biosynthesis · sugar nucleotides · UDP-galactose

- [1] a) L. Bode, *Glycobiology* **2012**, *22*, 1147–1162; b) H. Lagström, S. Rautava, H. Ollila, A. Kaljonen, O. Turta, J. Mäkelä, C. Yonemitsu, J. Gupta, L. Bode, *Am. J. Clin. Nutr.* **2020**, *111*, 769–778; c) P. K. Berger, J. F. Plows, R. B. Jones, T. L. Alderete, C. Yonemitsu, M. Poulsen, J. H. Ryoo, B. S. Peterson, L. Bode, M. I. Goran, *PLoS One* **2020**, *15*, e0228323.
- [2] M. Fajjes, M. Castejón-Vilatersana, C. Val-Cid, A. Planas, *Biotechnol. Adv.* **2019**, *37*, 667–697.
- [3] L. Bode, N. Contractor, D. Barile, N. Pohl, A. R. Prudden, G.-J. Boons, Y.-S. Jin, S. Jennewein, *Nutr. Rev.* **2016**, *74*.
- [4] K. Bych, M. H. Mikš, T. Johanson, M. J. Hederes, L. K. Vignæs, P. Becker, *Curr. Opin. Biotechnol.* **2019**, *56*, 130–137.
- [5] a) K. Parschat, S. Schreiber, D. Wartenberg, B. Engels, S. Jennewein, *ACS Synth. Biol.* **2020**, *9*, 2784–2796; b) L. Bode, N. Contractor, D. Barile, N.

- Pohl, A. R. Prudden, G. J. Boons, Y. S. Jin, S. Jennewein, *Nutr. Rev.* **2016**, *74*, 635–644.
- [6] a) Z. Xiao, Y. Guo, Y. Liu, L. Li, Q. Zhang, L. Wen, X. Wang, S. M. Kondengaden, Z. Wu, J. Zhou, X. Cao, X. Li, C. Ma, P. G. Wang, *J. Org. Chem.* **2016**, *81*, 5851–5865; b) H. Yu, X. Chen, *Org. Biomol. Chem.* **2016**, *14*, 2809–2818; c) D. Molnar-Gabor, M. J. Hederos, S. Bartsch, A. Vogel, <https://doi.org/10.1002/9783527813780>; d) K. Schmölzer, M. Lemmerer, A. Gutmann, B. Nidetzky, *Biotechnol. Bioeng.* **2017**, *114*, 924–928; e) J.-L. Fang, T.-W. Tsai, C.-Y. Liang, J.-Y. Li, C.-C. Yu, *Adv. Synth. Catal.* **2018**, *360*, 3213–3219; f) Y.-T. Huang, Y.-C. Su, H.-R. Wu, H.-H. Huang, E. C. Lin, T.-W. Tsai, H.-W. Tseng, J.-L. Fang, C.-C. Yu, *ACS Catal.* **2021**, *11*, 2631–2643.
- [7] a) T. F. T. Rexer, D. Laaf, J. Gottschalk, J. Frohnmeyer, E. Rapp, L. Elling in *Advances in Glycobiotechnology* (Eds.: E. Rapp, U. Reichl), Springer Nature, **2020**; b) B. Nidetzky, A. Gutmann, C. Zhong, *ACS Catal.* **2018**, *8*, 6283–6300.
- [8] a) D. Warnock, X. Bai, K. Autote, J. Gonzales, K. Kinealy, B. Yan, J. Qian, T. Stevenson, D. Zopf, R. J. Bayer, *Biotechnol. Bioeng.* **2005**, *92*, 831–842; b) L. Ruzic, J. M. Bolivar, B. Nidetzky, *Biotechnol. Bioeng.* **2020**, *117*, 1597–1602; c) J. Schmid, D. Heider, N. J. Wendel, N. Sperl, V. Sieber, *Front. Microbiol.* **2016**, *7*.
- [9] a) T. Bülter, L. Elling, *Glycoconjugate J.* **1999**, *16*, 147–159; b) Z. Liu, J. Zhang, X. Chen, P. G. Wang, *ChemBioChem* **2002**, *3*, 348–355.
- [10] Y. Zou, M. Xue, W. Wang, L. Cai, L. Chen, J. Liu, P. G. Wang, J. Shen, M. Chen, *Carbohydr. Res.* **2013**, *373*, 76–81.
- [11] J.-H. Lee, S.-W. Chung, H.-J. Lee, K.-S. Jang, S.-G. Lee, B.-G. Kim, *Bioprocess Biosyst. Eng.* **2009**, *33*, 71.
- [12] W. Finnigan, L. J. Hepworth, S. L. Flitsch, N. J. Turner, *Nat. Catal.* **2021**, *4*, 98–104.
- [13] C. Li, R. Zhang, J. Wang, L. M. Wilson, Y. Yan, *Trends Biotechnol.* **2020**, *38*, 729–744.
- [14] a) J. Yang, T. Zhang, C. Tian, Y. Zhu, Y. Zeng, Y. Men, P. Chen, Y. Sun, Y. Ma, *Biotechnol. Adv.* **2019**; b) K. Schmölzer, M. Weingarten, K. Baldenius, B. Nidetzky, *ACS Catal.* **2019**, *9*, 5503–5514; c) J. M. Sperl, V. Sieber, *ACS Catal.* **2018**, *8*, 2385–2396; d) R. A. Sheldon, D. Brady, *Chem. Commun.* **2018**, *54*, 6088–6104; e) R. Mahour, P. A. Marichal-Gallardo, T. Rexer, U. Reichl, *ChemCatChem* **2021**, *13*, 1–10.
- [15] a) I. Schomburg, L. Jeske, M. Ulbrich, S. Placzek, A. Chang, D. Schomburg, *J. Biotechnol.* **2017**, *261*, 194–206; b) I. Schomburg, A. Chang, D. Schomburg, *Nucleic Acids Res.* **2002**, *30*, 47–49.
- [16] a) R. Mahour, J. Klapproth, T. F. T. Rexer, A. Schildbach, S. Klamt, M. Pietzsch, E. Rapp, U. Reichl, *J. Biotechnol.* **2018**, *283*, 120–129; b) J. B. Thoden, H. M. Holden, *Protein Sci.* **2007**, *16*, 432–440.
- [17] R. J. Bayer, S. DeFrees, M. Ratcliffe (Ed.: USPTO), Neose Technologies Inc., USA, **1996**.
- [18] a) M. Pabst, J. Grass, R. Fischl, R. Léonard, C. Jin, G. Hinterkörner, N. Borth, F. Altmann, *Anal. Chem.* **2010**, *82*, 9782–9788; b) M. Melmer, T. Stangler, A. Premstaller, W. Lindner, *J. Chromatogr. A* **2011**, *1218*, 118–123; c) T. E. Bapiro, F. M. Richards, D. I. Jodrell, *Anal. Chem.* **2016**, *88*, 6190–6194; d) A. Ndiripo, A. Albrecht, H. Pasch, *RSC Adv.* **2020**, *10*, 17942–17950; e) D. Kot, M. Zou, K. Brunnengräber, J.-H. Arndt, T. Macko, B. J. M. Etzold, R. Brüll, *J. Chromatogr. A* **2020**, *1625*, 461302.
- [19] S. Koizumi, T. Endo, K. Tabata, A. Ozaki, *Nat. Biotechnol.* **1998**, *16*, 847–850.
- [20] T. Fischöder, D. Laaf, C. Dey, L. Elling, *Molecules* **2017**, *22*, 1320.
- [21] a) J. S. Hawkes, R. A. Gibson, D. Robertson, M. Makrides, *Eur. J. Clin. Nutr.* **2006**, *60*, 254–264; b) D. Lecca, S. Ceruti, *Biochem. Pharmacol.* **2008**, *75*, 1869–1881; c) T. W. Kensler, D. A. Cooney, in *Advances in Pharmacology*, Vol. 18 (Eds.: S. Garattini, A. Goldin, F. Hawking, I. J. Kopin, R. J. Schnitzer), Academic Press, **1981**, pp. 273–352; d) A. F. Hadfield, A. C. Sartorelli, in *Advances in Pharmacology*, Vol. 20 (Eds.: S. Garattini, A. Goldin, F. Hawking, I. J. Kopin, R. J. Schnitzer), Academic Press, **1984**, pp. 21–67.
- [22] M. Doi, Y. Tsunemi, S. Asahi, *Biosci. Biotechnol. Biochem.* **1994**, *58*, 1608–1612.
- [23] H. Wu, Y. Li, Q. Ma, Q. Li, Z. Jia, B. Yang, Q. Xu, X. Fan, C. Zhang, N. Chen, X. Xie, *Metab. Eng.* **2018**, *49*, 248–256.
- [24] a) T. Shintani, *Fermentation* **2019**, *5*, 47; b) S. T. Yang, E. M. Silva, *J. Dairy Sci.* **1995**, *78*, 2541–2562.
- [25] a) H. L. Mudoga, H. Yucel, N. S. Kincal, *Bioresour. Technol.* **2008**, *99*, 3528–3533; b) S. Zhang, T. Shao, H. S. Kose, T. Karanfil, *Environ. Sci. Technol.* **2010**, *44*, 6377–6383; c) L. Wang, Y. Yao, Z. Zhang, L. Sun, W. Lu, W. Chen, H. Chen, *Chem. Eng. J.* **2014**, *251*, 348–354.
- [26] J. H. Knox, B. Kaur, G. R. Millward, *J. Chromatogr. A* **1986**, *352*, 3–25.
- [27] a) K. R. Echols, R. W. Gale, K. Feltz, J. O’Laughlin, D. E. Tillitt, T. R. Schwartz, *J. Chromatogr. A* **1998**, *811*, 135–144; b) C. West, C. Elfakir, M. Lafosse, *J. Chromatogr. A* **2010**, *1217*, 3201–3216; c) P. Chaimbault, K. Petritis, C. Elfakir, M. Dreux, *J. Chromatogr. A* **2000**, *870*, 245–254.
- [28] a) S. T. Kulmer, A. Gutmann, M. Lemmerer, B. Nidetzky, *Adv. Synth. Catal.* **2017**, *359*, 292–301; b) M. Lemmerer, K. Schmolzer, A. Gutmann, B. Nidetzky, *Adv. Synth. Catal.* **2016**, *358*, 3113–3122.
- [29] a) C. Li, L.-X. Wang, *Chem. Rev.* **2018**, *118*, 8359–8413; b) L. Van Landuyt, C. Lonigro, L. Meuris, N. Callewaert, *Curr. Opin. Biotechnol.* **2019**, *60*, 17–28; c) W. Kightlinger, K. F. Warfel, M. P. Delisa, M. C. Jewett, *ACS Synth. Biol.* **2020**, *9*, 1534–1562; d) M. Thomann, T. Schlothauer, T. Dashivets, S. Malik, C. Avenal, P. Bulau, P. Rüger, D. Reusch, *PLoS One* **2015**, *10*; e) T. F. T. Rexer, L. Wenzel, M. Hoffmann, S. Tischlik, C. Bergmann, V. Grote, S. Boecker, K. Bettenbrock, A. Schildbach, R. Kottler, R. Mahour, E. Rapp, M. Pietzsch, U. Reichl, *J. Biotechnol.* **2020**, *322*, 54–65; f) T. F. T. Rexer, A. Schildbach, J. Klapproth, A. Schierhorn, R. Mahour, M. Pietzsch, E. Rapp, U. Reichl, *Biotechnol. Bioeng.* **2018**, *115*, 192–205; g) V. S. Tayi, M. Butler, *Biotechnol. J.* **2018**, *13*.
- [30] M. C. C. Bustamante, M. O. Cerri, A. C. Badino, *Chem. Eng. Sci.* **2013**, *90*, 92–100.

---

Manuscript received: July 22, 2021

Revised manuscript received: October 10, 2021

Accepted manuscript online: October 12, 2021

Version of record online: December 14, 2021